Available online at www.eccomasproceedia.org
Eccomas Proceedia COMPDYN (2019) 4748-4767

ECCOMAS
Proceedia

COMPDYN 2019
7th ECCOMAS Thematic Conference on
Computational Methods in Structural Dynamics and Earthquake Engineering
M. Papadrakakis, M. Fragiadakis (eds.)
Crete, Greece, 24–26 June 2019

NONLINEAR DYNAMIC RESPONSES OF HIGHWAY BRIDGES EXPOSED TO PARTICULAR SEISMIC EVENTS CONSIDERING VEHICLE-BRIDGE INTERACTIONS

Sudanna Borjigin[1], Chul-Woo Kim[2], Kai-Chun Chang[2] and Kunitomo Sugiura[2]

[1] CORE Institute of Technology Corporation
Osaka JA Building 4F, 1 Chome 2-5 Nishitenma, Kita-ku, Osaka-shi, Osaka- Fu 530-0047, Japan
s.borjigin@coreit.co.jp

[2] Department of Civil and Earth Resources Engineering, Graduate School of Engineering
Kyoto University
Kyotodaigaku-katsura, Nishikyo-ku, Kyoto 615-8540, Japan
{kim.chulwoo.5u, chang.kaichun.4z, sugiura.kunitomo.4n}@kyoto-u.ac.jp

Abstract

The highway bridge design code in most countries does not consider the live load in seismic design of highway bridges. However, traffic jams on urban highway bridges occur with high probability, and the inertial effect of passing vehicles due to earthquakes thus could not be negligible in the context of seismic design of bridges when vehicle's weight is large enough compared with the dead load of bridges. It is therefore of engineers' interest to conduct a seismic analysis of bridges considering the vehicle dynamics effect on the seismic behavior of the bridge. Earthquakes occur unexpectedly and recently more and more strong motions were recorded, which are important for seismic engineering. This paper investigates nonlinear dynamic responses of a highway bridge considering vehicle‑bridge interactions (VBI) subjected to particular large earthquakes: Tohoku earthquake in 2011 and Kumamoto earthquake in 2016. Observations showed that, compared with those of disregarding vehicles, VBI changed the bridge displacement responses, plastic deformations, relative displacements of bearings and acceleration responses of the bridge but to different tendency and degree under different ground motions. The results revealed the importance of vehicle dynamic effect on seismic responses of bridges and view point that the current assumption of ignorance of vehicle effect in seismic design of highway bridges might be non-conservative.

Keywords: Bridge Non-linear Behavior, Moving Vehicle, Particular Earthquakes, Seismic Analysis, Vehicle‑bridge Interaction.

ISSN:2623-3347
Peer-review under responsibility of the organizing committee of COMPDYN 2019.
doi: 10.7712/120119.7265.19891

1 INTRODUCTION

Earthquakes occur randomly and such strong motion records are important for seismic design. On March 11, 2011, the 2011 off the Pacific Coast of Tohoku Earthquake (hereafter, the "Tohoku Earthquake") occurred in Japan. The magnitude was reported as being 9.0, the highest magnitude ever recorded in Japan. It was the most powerful earthquake ever recorded to have hit Japan, and the scale of the Tohoku Earthquake stands out in comparison even with some of the most destructive past earthquakes. It caused enormous damage due to the ground motion and the tsunami it triggered. About 200 highway bridges and numerous railway bridges were damaged, e.g., elevated bridges of the Tohoku Shinkansen. The Tohoku Earthquake was an inter-plate earthquake, occurring on the boundary between the Pacific plate and the Continental plate. The observed ground motions had a typical characteristic of a long duration because of the large scale of the fault plane, or the large number of waveforms observed, which was higher than massive earthquakes in the past. This phenomenon caused severe liquefaction effects for the ground in the Tokyo Bay area. Liquefaction resulted in much of the destruction associated with this earthquake, such as sand/mud boiling, ground cracking, depressions of pavement, ground settlement, leaning buildings and the exposure of underground pipes. The Kumamoto earthquake in 2016 consists of two strong ground motions and a series of smaller foreshocks and aftershocks. The first large ground motion hit the area on April 14, 2016, which was categorized into the foreshock before the larger ground motion on April 16, 2016. Such earthquakes caused strong response and significant damage to bridges. It was mentioned that this type of repeated strong motions has not been taken into account in conventional seismic design practices [1]. The repeated strong motions increase damage in all types of structures significantly. Service on the Shinkansen was suspended after a train derailed due to the earthquake. Thus, more research is needed to estimate and prevent the damage caused by such strong earthquakes.

Heavy traffic jams on urban highway bridges occur frequently and encountering an earthquake in urban areas of earthquake prone regions becomes more possible. The dynamic effect of vehicles could not be negligible in the context of seismic design of bridges. It is necessary to review the seismic performance of bridges, considering traffic loading. However, very few studies have specifically examined the vehicle effect on bridge seismic responses.

In seismic design of monorail bridges the effect of the train load is considered as additional mass [2]. He et al. [3] investigated the seismic responses of Shinkansen viaducts for high-speed trains under moderate earthquakes. Their results show that the train can act as a damper for the bridge. A study by Zeng and Dimitrakopoulos [4] studied a horizontally curved railway bridge subjected to train crossings and moderate ground motions of different periods. Results verified the favorable damping effect that the running vehicles have on the deck vibration. The study by Kim et al. [2] showed that consideration of the monorail train as additional mass rather than a dynamic system in numerical modeling overestimated the effect of the train load on seismic performance of monorail bridges. Kim and Kawatani [5] concluded that a train acts as a damper and tends to decrease acceleration response under a particular earthquake compared with the system which consider train as an additional mass.

In contrast to the railway system, the highway bridge design code of Japan Road Association does not consider the live load in seismic design of highway bridges due to the low probability of simultaneously encountering critical vehicle load and earthquake. A study by Sugiyama et al. [6] showed that the dynamic effect of the vehicles was more dominant in the transverse direction and that the vehicle loading tended to reduce the bridge response. A study addressing this matter was done by Kameda et al. [7], which concluded that seismic responses of the bridge increase or decrease depending on the phase difference between the bridge and the vehicle. Kameda et al. [8] stated that the vehicles tended to amplify the bridge response when the vehicles and bridge were in phase and tended to decrease the response when they were out of phase. Another study by Kim et al. [9] concluded that the seismic response of the highway bridge subject to moderate earthquakes increased when the vehicle was considered as mass; and decreased when the vehicle was simulated as dynamic system. Kawatani et al. [10] demonstrated that heavy vehicles reduced the seismic response of bridges under a moderate ground motion with lower frequency characteristics; but slightly amplified the seismic response of the bridge under higher frequency ground motions. Borjigin et al. [11] proposed a seismic response analysis framework incorporating vehicle–bridge interactions (VBI) with nonlinear dynamic analysis, and the effects of vehicle dynamics on seismic responses of a highway bridge was clarified and the seismic performance of the bridge was checked.

As reviewed above, most studies were related to moderate earthquakes that caused linear behavior of bridges, and some studies discussed the seismic responses of bridges considering effect of vehicle dynamics under limited number of modified ground motions. It is therefore necessary to proceed with a seismic analysis of bridges considering vehicle effect, and describe the non-behavior of bridges for strong ground shakings of different levels. This study was conducted to investigate non-linear dynamic analysis incorporating vehicle–bridge interactions (VBI) subjected to particular earthquakes to clarify the effect of vehicles on the seismic responses of an urban highway viaduct. To investigate the seismic responses of the bridge under particular earthquakes, two strong ground motions recorded on-site with different frequency components are adopted for analysis. A numerical method, Recursive Substructure Method, was utilized, which integrates a commercial FEA package, ABAQUS®, into the authors' in-house VBI-solving programs developed with MATLAB®.

2 ANALYTICAL MODELS

2.1 Vehicle model

The vehicle model of a truck consists of a rigid body with single axle. The mass of the vehicle model is 25.0 ton. The vehicle model has five degree of freedoms (DOFs) considering transversal, longitudinal, vertical, pitching, and rolling motions as shown in Figure 1. The properties are shown in Table 1. The length of truck is 7 m. The natural frequency of longitudinal motion of the vehicle model is about 2.052 Hz. The slip or turning over of vehicles on the bridge during the earthquakes was not considered in this study.

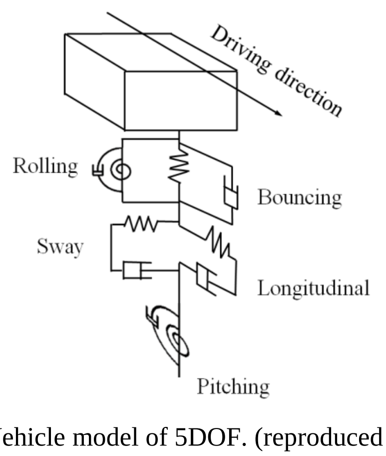

Figure 1: Vehicle model of 5DOF. (reproduced from [11])

	Natural frequency	Spring constant	Damping coefficient
Transversal & longitudinal	2.052 Hz	4.156×10^{6} N/m	4.284×10^{4} N·s/m
Vertical	3.477 Hz	1.193×10^{7} N/m	5.871×10^{4} N·s/m
Pitching	2.697 Hz	2.326×10^{7} N·m/rad	1.505×10^{5} N·m·s/rad
Rolling	1.739 Hz	9.665×10^{6} N·m/rad	4.756×10^{4} N·m·s/rad

Table 1: Properties of 5DOF vehicle model. (reproduced from [11])

2.2 Bridge model

The target bridge was designed in 2009 according to the design specifications for the Japan highway bridges. The bridge model (Figure 2) used in this study was a 3-span continuous non-composite steel plate girder bridge with two vehicle lanes. The superstructure of the bridge model contains an orthotropic plate supported by five girders. The girders, reinforced concrete (RC) piers and abutments were modelled with beam elements and the plate was modeled with shell elements. The properties of cross section and mechanical properties are given in Table 2 and Table 3. Rayleigh damping was adopted [12].

Strong earthquakes may cause non-linear behaviors of bridges. The failure mode of this bridge was predicted to be in the longitudinal direction. The bridge included isolation bearings of bi-linear force-displacement relationship on each abutment and pier (Table 4) which moved in the longitudinal direction, and plastic hinges of tri-linear moment-rotation relationships on the piers base (Table 5) which rotated along the transversal axis. The abutments were made of concrete and performed linear behavior, while the piers were made of reinforced concrete and performed non-linear behavior.

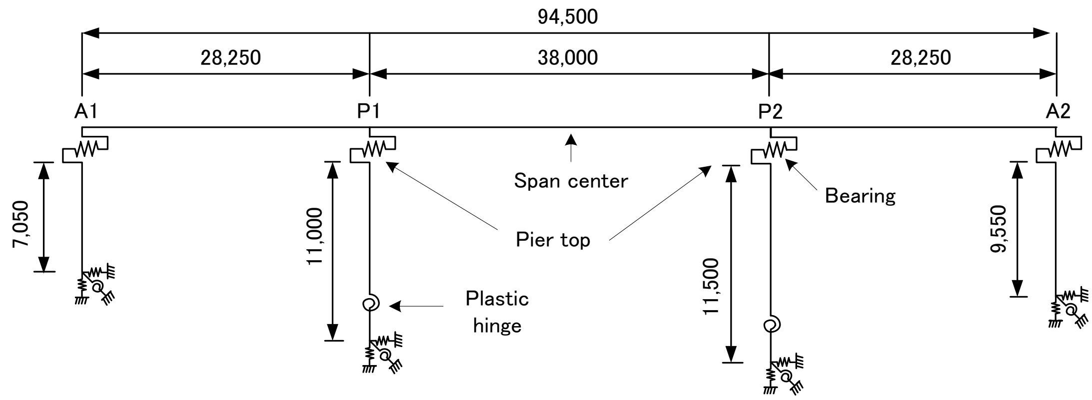

Figure 2: Analytical model of bridge (unit: mm). (reproduced from [11])

Component		Section area A (m^2)	Second moment of area Iz (m^4)	Second moment of area Ix (m^4)	Torsional constant J (m^4)
Girder		0.658	0.363	4.65820	0.0075
Abutment 1 (A1)	Column	33.375	17.383	495.700	61.260
	Footing*	10000	10000	10000	10000
Pier 1 (P1)	Bent cap*	10000	10000	10000	10000
	Column	12	4.41870	36	12.643457
	Plastic zone	12	10000	10000	10000
	Footing*	10000	10000	10000	10000
Pier 1 (P2)	Bent cap*	10000	10000	10000	10000
	Column	12	4.41870	36	12.643457
	Plastic zone	12	10000	10000	10000
	Footing*	10000	10000	10000	10000
Abutment 2 (A2)	Column	33.375	17.383	495.700	61.260
	Footing*	10000	10000	10000	10000

Note. * The unrealistic value 10000 was assigned herein simply for providing a relatively large rigidity.

Table 2: Properties of cross section main components. (reproduced from [11])

	Young's modulus E (N/m^2)	Shear modulus G (N/m^2)	Density (kg/m^3)
Girder	2.0×10^{11}	7.7×10^{10}	7857
Pier	2.5×10^{10}	–	2500

Table 3: Mechanical properties of the bridge model. (reproduced from [11])

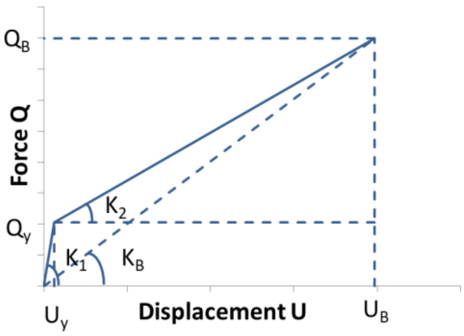

	A1	P1	P2	A2
K_1(kN/m)	16304.2	38371	38233	16373.8
K_2 (kN/m)	1545.6	3645.0	3632.2	1551.8
Q_y (kN)	102.39	214.88	213.34	102.66
Q_B (kN)	399.33	718.98	708.84	404.22
U_y (m)	0.006	0.006	0.006	0.006
U_B (m)	0.198	0.144	0.142	0.201
K_B(kN/m)	2013.03	4996.36	4992.75	2014.85

Note. K_1 denotes the initial stiffness, K_2 the post yielding stiffness, K_B the equivalent stiffness, and (U_y, Q_y) and (U_B, Q_B) indicates initial yielding point (yielding shear deformation and force) and ultimate point (yielding ultimate shear deformation and force) respectively.

Table 4: Properties of bearings. (reproduced from [11])

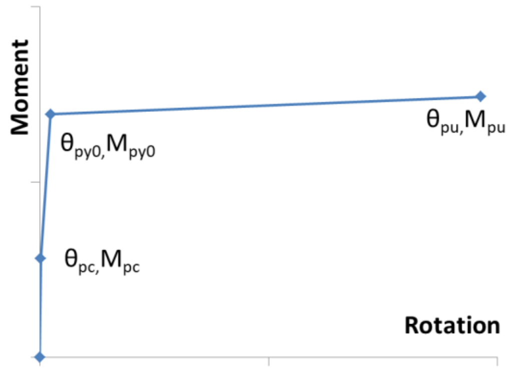

	P1	P2
M_{pc} (kN·m)	11297.8	11377.3
M_{py0} (kN·m)	27749.3	27928.4
M_{pu} (kN·m)	29725.7	29838.9
θ_{pc} (rad)	0.000103	0.000103
θ_{py0} (rad)	0.001192	0.001198
θ_{pu} (rad)	0.048174	0.047547

Note. Initial cracking moment M_{pc} and its corresponding rotational angle θ_{pc} specifies the initial cracking point and elastic limit, the yielding moment M_{py0} and rotation angle θ_{py0} specifies the yielding point, the ultimate moment M_{pu} and rotation angle θ_{pu} specifies the ultimate point.

Table 5: Properties of plastic hinge. (reproduced from [11])

The road condition was considered to be good in this study. The roadway profile generated based on ISO standard [13] is shown in Figure 3. Usually effects of vehicle vibrations actuated during moving on a bridge by road roughness are relatively small compared with seismic load effects. However, before an earthquake bridge vibration is mainly excited by vehicle vibrations, and the bridge vibration due to moving vehicles can be applied as initial conditions in the dynamic analysis of bridges during earthquakes. Before seismic responses, the responses by vehicles only should be identified. Therefore, this study considers the road roughness in the analysis [9].

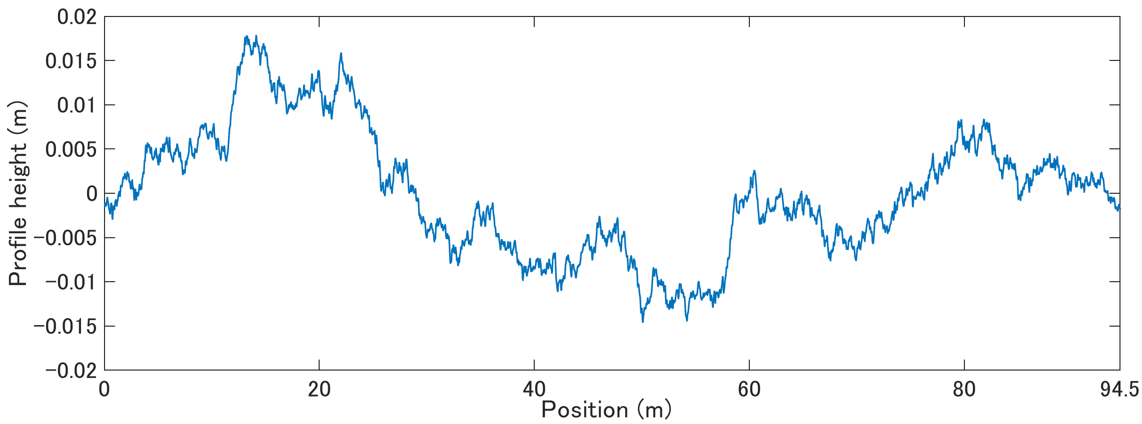

Figure 3: Road roughness profile. (reproduced from [11])

Since the vehicle position on the bridge varies with time, the natural frequency of bridge with vehicles standing at different loading locations were examined through eigenvalue analysis of the vehicle-bridge interactive system. There were five vehicles equally spaced on each lane and totally ten vehicles were considered in the VBI system. The natural frequency of the first longitudinal mode of the bridge without vehicle was 1.82 Hz. Position 1 (see Table 6) is a special condition with 2 vehicles exactly standing on the top of two piers on each lane. As shown in Table 6, the first mode is piers' longitudinal bending and rubber bearings' deformation mode. Two longitudinal modes and frequencies of the vehicle-bridge interactive system corresponds to the first longitudinal mode: vehicles in-phase (vehicles move in the same direction as the bridge's movement) and out-of-phase (vehicles move in the opposite direction of the bridge's movement) with the bridge, with the frequency of 1.43 Hz and 2.02 Hz, respectively. Position 2 (Table 6) is one vehicle standing on the top of left abutment on each lane, while Position 3 (Table 6) is one vehicle standing on the top of right abutment on each lane and symmetrical with Position 2. For this reason, the discussion with position 3 scenario is omitted in following sections. With position 2 and 3, frequency of vehicles in-phase mode is 1.17 Hz and that of out-of-phase mode is 1.89 Hz. Position 4 (Table 6) is a random position different from the above 3 ones. Frequency of vehicles in-phase mode is 1.35 Hz and that of out-of-phase mode is 1.97 Hz.

It can be found that the bridge has varied fundamental natural frequencies as the vehicles were moving on the bridge. Due to the presence of vehicles, the frequency of the bridge may be changed to be larger or smaller than that of bridge alone, e.g. at position 1 the frequency of vehicles in-phase mode is 1.43 Hz that is smaller than the natural frequency of the first mode of bridge alone 1.82 Hz, while frequency of out-of-phase mode is 2.02 Hz, which is larger than the natural frequency of the first mode of bridge alone 1.82 Hz. Such frequency variation may significantly cause change in seismic responses of the bridge, as discussed below.

Bridge without vehicle	Bridge with 10 vehicles (position 1)	Bridge with 10 vehicles (position 2,3)	Bridge with 10 vehicles (position 4)
	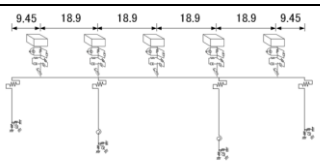	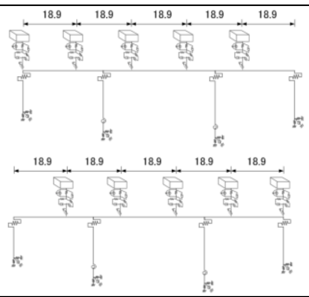	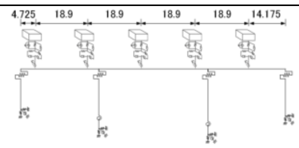
1.82 Hz 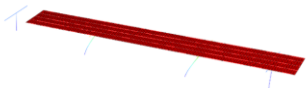	vehicles in phase with the bridge 1.43 Hz 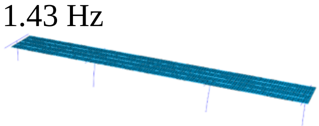 vehicles out of phase with the bridge 2.02 Hz 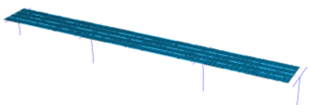	vehicles in phase with the bridge 1.17 Hz 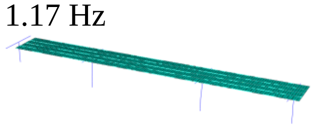 vehicles out of phase with the bridge 1.89 Hz 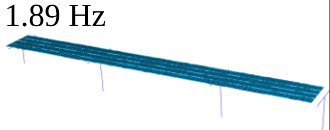	vehicles in phase with the bridge 1.35 Hz 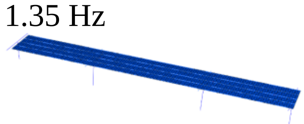 vehicles out of phase with the bridge 1.97 Hz 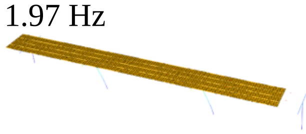

Table 6: Comparison of natural frequencies and mode shapes of the bridge based on equivalent stiffness without vehicle and with vehicles standing on different positions. (reproduced from [11])

2.3 Moving vehicle configuration

To investigate the effect of moving vehicles on the seismic response of the highway viaduct, the following scenario was considered. Figure 4 shows the moving pattern of heavy vehicles. It was assumed that the earthquake happened when the bridge was fully loaded with moving vehicles. In other words, only the seismic response of the bridge fully loaded by moving vehicles is discussed in this study. All vehicles are assumed to travel with the constant speed of 2.7 m/s (9.72 km/h). The spacing between adjacent vehicles is 18.9 m. Comparing the responses in this scenario with another scenario, disregarding vehicular loadings, can be useful to elucidate the effects of continuously moving vehicles.

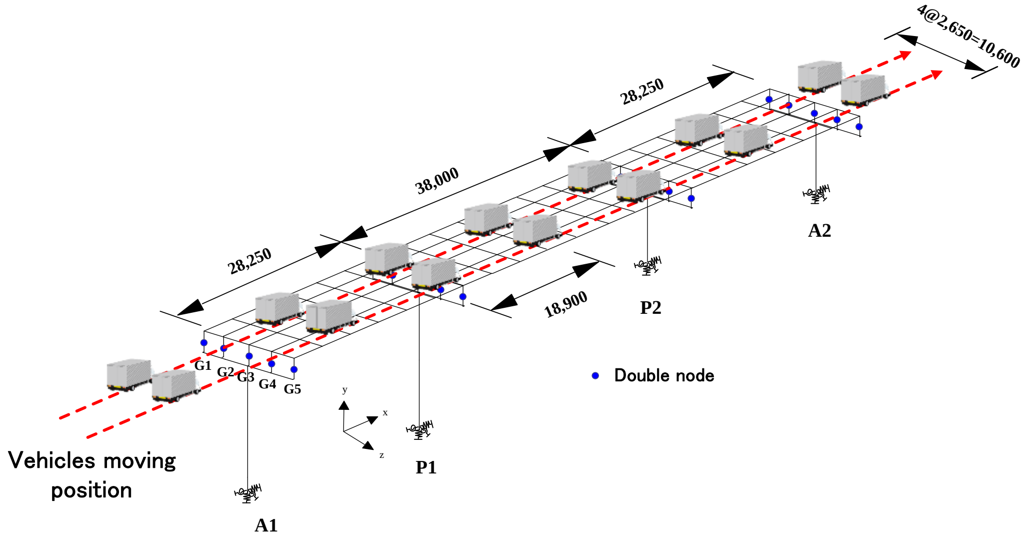

Figure 4: The bridge model with continuously moving vehicles. (reproduced from [11])

3 GROUND MOTIONS

Two particular ground motions were considered herein: 2011 Tohoku earthquake and 2016 Kumamoto earthquake. Their characteristics are given as follows.

3.1 Tohoku earthquake

The strong ground motion records of Tohoku earthquake clearly showed that this earthquake generated ground motions with multiple pulses and longer duration, compared to the 1995 Kobe Earthquake lasting about 20 seconds. Figure 5 shows the time history of Kaihoku Bridge, Ishinomaki EW component, a modified ground motion of Level 2 Type I recommended by JRA [14] used herein, which was obtained from the recorded ground motion in the Tohoku earthquake at the measurement station of Kaihoku Bridge, Ishinomaki. The designation of EW indicates data channels of East-West direction. The Level 2 ground motion indicates the extreme design ground motion with low occurrence probability such as Kobe earthquake in 1995 and Type I indicates inter-plate earthquakes. For the highway bridge adopted in this analysis, the ground condition is classified as Group I soil in the design code, which is defined as dense to stiff soil having a natural period of 0.16 – 0.6 s in the surface ground.

As shown in Figure 5, the ground motion contains two attacks with a spacing of about 50 seconds and lasts for about 240 seconds. The first attack has smaller peak value of acceleration (5.12 m/s^2) than the second attack does (7.95 m/s^2). The figure shows a drastic change in amplitude and spike-like phases, which all corresponds to the characteristics of the records on the liquefied ground. The sampling frequency is 100 Hz.

Figure 6 shows the acceleragram, Fourier amplitude spectrum and pseudo acceleration response spectrum (damping ratio h = 0.05) of the modified ground motion. The modified ground motion was obtained by fitting its response spectrum to the target response spectrum. Periods (and frequencies) in the legend of response spectrum and Fourier amplitude spectrum are natural periods (frequencies) of vehicle's longitudinal mode, the first natural periods (frequencies) of the bridge's longitudinal modes disregarding vehicles and regarding vehicles as dynamic system (at Position 1, 2 and 4) respectively.

For computation efficiency, a shorter ground motion (referred to as GM1 hereafter) was extracted from the 20th to 140th second of the full record and then applied to the aforementioned VBI model. The ground motion was applied in the longitudinal direction because the piers' bending resistance is weakest in this direction according to the formal design.

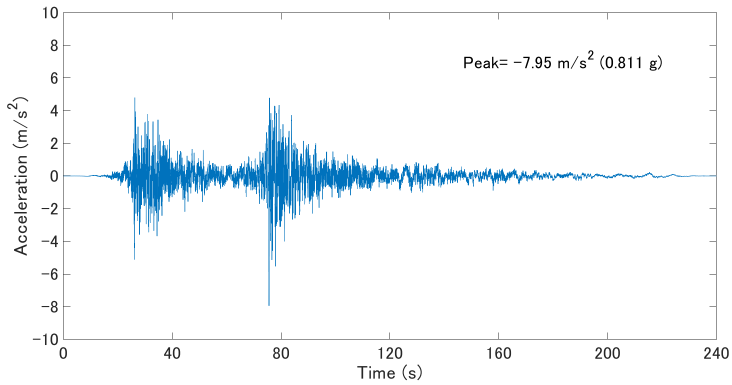

Figure 5: Kaihoku Bridge, Ishinomaki EW component (GM1).

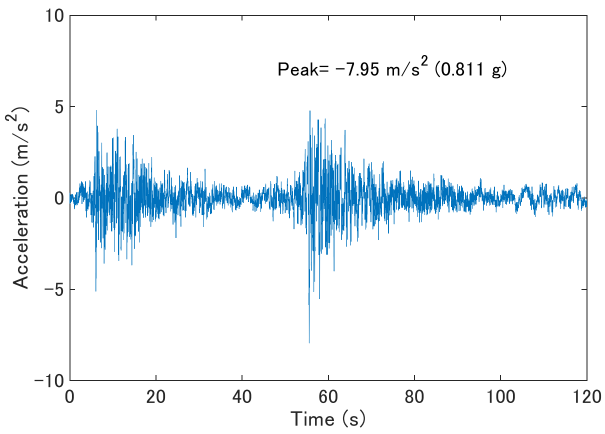

(a)

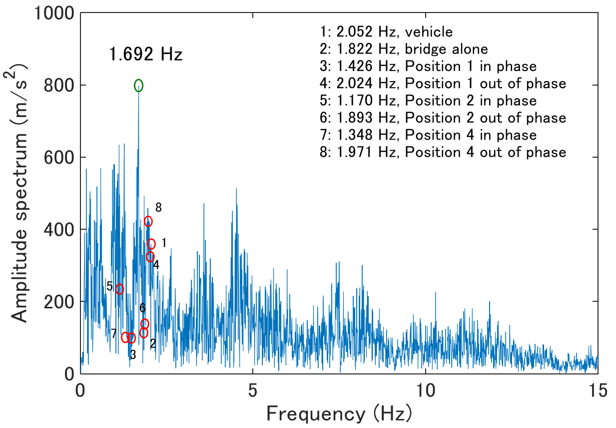

(b)

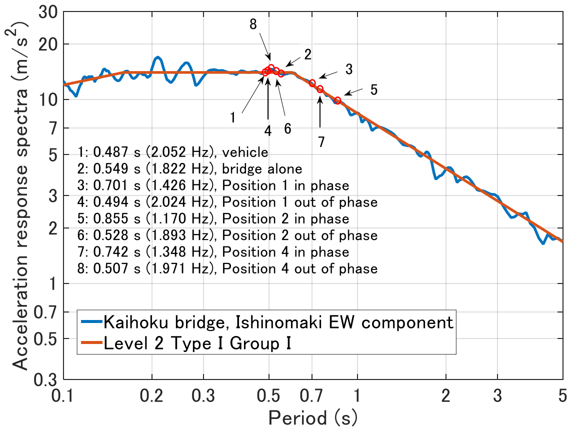

(c)

Figure 6: Accelerogram, response spectrum and Fourier spectrum of strong shaking interval (20 s ~ 140 s) of Kaihoku Bridge EW component (GM1): (a) accelerogram, (b) Fourier amplitude spectrum, (c) pseudo acceleration response spectrum.

3.2 Kumamoto earthquake

Figure 7 shows the acceleration time histories of the NS and EW components of the ground motion recorded at Mashiki town (referred to as GM2 hereafter) [15]. The strong motion record above the heavily damaged Mashiki residential area recorded over 1.0g in the EW direction. The designations of EW and NS in the figures, respectively, indicate data channels of East-West, North-South directions. The maximum acceleration is 6.53 m/s^2 in the NS component and 11.57 m/s^2 in the EW component. In the seismic analysis, EW component was applied to the longitudinal direction and NS was applied to the transverse direction of the bridge structure.

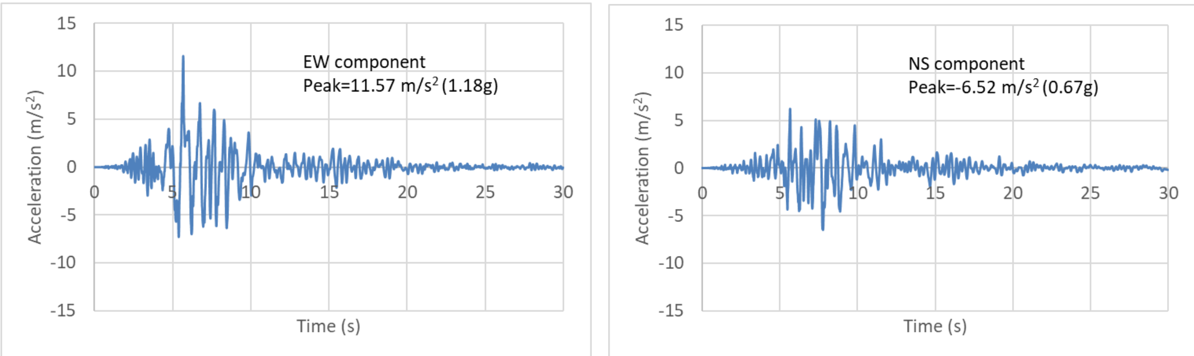

Figure 7: Accelerogram of Mashiki town EW component and NS component (GM2).

4 NUMERICAL METHOD

The equation of motion for a vehicle is written as [16] [17]

$$\boldsymbol{M}_v\ddot{\boldsymbol{u}} + \boldsymbol{C}_v(\dot{\boldsymbol{u}} - \dot{\boldsymbol{y}}_c) + \boldsymbol{K}_v(\boldsymbol{u} - \boldsymbol{y}_c) = \boldsymbol{0} \quad (1)$$

where $\boldsymbol{M}_v$, $\boldsymbol{C}_v$, and $\boldsymbol{K}_v$ respectively denote the mass, damping, and stiffness matrices of the vehicle, and where $\boldsymbol{u}$ represents the vector of vehicle's displacements and rotations at its degrees of freedom. A dot denotes the derivative with respect to time. $\boldsymbol{y}_c$ is the wheel displacement vector at the contact point. It is the summation of bridge displacement $\boldsymbol{w}_c$ and roughness $\boldsymbol{r}_c$ at that point.

The equation of motion for the bridge model is written as

$$\boldsymbol{M}_b\ddot{\boldsymbol{v}} + \boldsymbol{C}_b\dot{\boldsymbol{v}} + \boldsymbol{K}_b\boldsymbol{v} = \boldsymbol{f}_{seis} + \boldsymbol{f}_{vb} \quad (2)$$

where $\boldsymbol{M}_b$, $\boldsymbol{C}_b$ and $\boldsymbol{K}_b$ respectively stand for the mass, damping, and stiffness matrices of the bridge, and where $\boldsymbol{v}$ represents the vector of bridge's displacements and rotations at its degrees of freedom. Also, $\boldsymbol{f}_{seis}$ is the seismic loading. The force exerted by vehicle to bridge $\boldsymbol{f}_{vb}$ is the summation of vehicle weight, spring forces, and damping forces.

The two equations of motion (1) and (2) above are solved in a direct time integration manner to solve them at a certain time step $t+\Delta t$ (Δt is a finite small time increment) using the solution in previous time step t and the approximations for the derivatives. Newmark β-method [26] is adopted to solve equations of the equations of the vehicle and bridge system. The value of 0.25 is adopted for β to obtain stable and accurate solutions.

The Recursive Substructure Method (RSM) [11] was utilized to simulate the dynamic responses of bridges and moving vehicles under particular earthquake [18] [19]. It integrates the conventional nonlinear dynamic analysis in ABAQUS into the authors' in-house VBI-solving programs developed with MATLAB. The bridge Finite Element model is built in ABAQUS, and nonlinear dynamic analysis of bridge is conducted in ABAQUS. The vehicle model is built and the roughness profile is constructed in MATLAB. MATLAB controls the recursive ABAQUS executions and to perform time integrations in VBI problem. The time step of simulations was 0.01 s, being the same as the sampling period of the ground motion record.

5 SEISMIC RESPONSES OF HIGHWAY BRIDGE

5.1 Displacement responses of pier top and relative displacement of bearing

The shear force-displacement hysteresis loops of bearing, the longitudinal displacement responses of pier top and the moment-rotation hysteresis loops at pier base of P1 under GM1 are depicted in Figures 8-10 as typical example, and those of A1, P2 and A2 are omitted here for simplicity. As shown in Figure 9, the maximum displacement of pier top P1 under GM1 is about 0.04 m during first attack, and nonlinear behavior happened that caused a drift in the response of approximately 0.01 m. There is very little difference between the results with and without vehicle during the first attack. However, during the following second attack, which is like a strong aftershock of the first attack, the maximum displacement of the bridge appears and the displacement responses under second attack have larger amplitudes than those during first attack. From this phenomenon the larger residual displacement can be predicted. It is noteworthy that significant difference between two scenarios disregarding and regarding vehicles in the second attack could be found and the moving vehicles tend to reduce the displacement responses of the bridge, which indicates the presence of vehicles mitigates the variation tendency of the displacement response of the bridge while subjected to multi-attacks ground motions.

The relative displacements of bearings considering VBI under GM1 were slightly changed from those disregarding vehicles as indicated in Figure 8 and Table 7. The maximum relative displacements decreased by 0.6% for A1, by 3.8% for P1 and by 0.8% for P2, but increased by 2.4% at A2. The reason may be added damping and mass damper effect due to vehicle on the bridge. Another reason may be that the vehicle-bridge out-of-phase modes were excited by the ground motion and the vehicle's suspension system would suffer a larger deformation and dissipate more energy that was supposed to be dissipated by the rubber bearings. For example, the natural frequency of the vehicle-bridge out-of-phase mode in the Position 4 scenario is 1.971 Hz and it might be excited by the ground motion as indicated in Figure 6(b), and the out-of-phase mode might be excited by the ground motion. It can be said that the current seismic design disregarding vehicle dynamics was conservative if the rubber bearings were of concern.

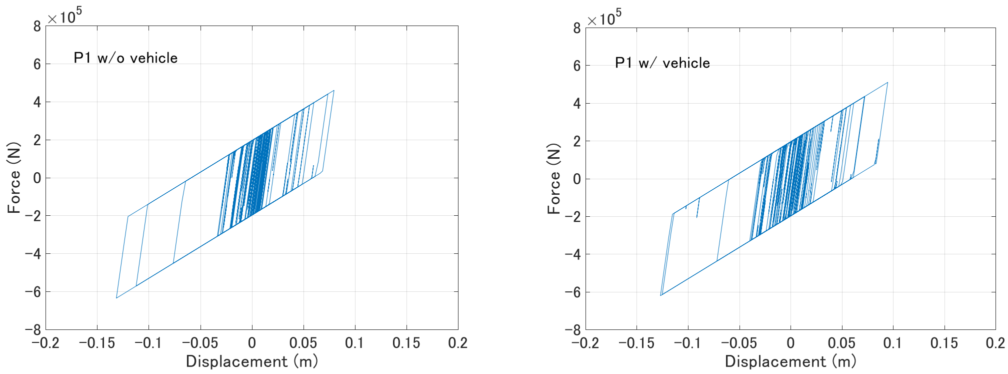

Figure 8: Hysteresis loop of bearing at P1 pier top under GM1, disregarding moving vehicles (left) and considering moving vehicle (right).

		Displacement	Reduction ratio * %
A1	w/o	0.164	0.6
	w/	0.163	
P1	w/o	0.132	3.8
	w/	0.127	
P2	w/o	0.126	0.8
	w/	0.125	
A2	w/o	0.168	-2.4
	w/	0.172	

Note. *reduction ratio is defined as the average displacement reduction from the w/o-vehicles case to the w/-vehicles case divided by the average displacement in the w/o-vehicles case.

Table 7: Maximum relative displacement of bearing under GM1 (unit: m).

The maximum longitudinal displacements of span center under GM1 were reduced when the moving vehicles presented by 1.8% as indicated in Table 8. Span center displacement is the summation of pier top displacement and bearing's relative displacement. Referring to Table 7 and 8, the span center maximum displacements and the bearing's maximum relative displacements are at a similar level (0.12 – 0.17 m), while the span center maximum displacements and the pier top maximum displacements (only about 0.06 m from Figure 9) are not. It indicates that the span center maximum displacements were more dominated by bearings' maximum relative displacements. As mentioned above, when the vehicles were considered on the bridge system, two modes appeared relevant to the first longitudinal mode of the bridge alone: vehicle-bridge in-phase and out-of-phase modes. Although the out-of-phase modes were excited by the ground motions to a similar level with the original bridge-alone mode was (see the pseudo acceleration response spectrum in Figure 6(c)), the phase-difference between vehicles and bridge might help bearings absorb energy and therefore reduce the bearings' relative displacements as well as the span center displacements.

The maximum displacements of pier tops were generally reduced when the moving vehicles presented (see Figure 9), and so were the residual displacements of pier tops as well as span center. Such ground motion caused the maximum displacement up to about 0.066 m and the residual displacement about 0.03 m at pier tops. But if vehicle-bridge interaction was considered, the reduction for maximum displacements was up to 19% and for residual displacement responses was 36%. The maximum displacement decreased by 13.8% at P1 pier top and 19.3% at P2 pier top; the residual displacement decreased by 31.6% at P1 pier top, 35.9% at P2 pier top, and 21.4% at span center, when vehicle–bridge interaction was considered. It could be concluded that the vehicles have a significant positive effect on the bridge's nonlinear displacement responses. When the moving vehicles were considered, the maximum rotation of the plastic hinge at pier base was smaller than those without vehicle under the ground motion (see the moment-rotation hysteresis loops in Figure 10), indicating that the bridge suffered from weaker plastic deformations. Table 9 quantifies the reduction of the maximum rotation: 37.5% at P1 pier base and 39.3% at P2 pier base. This trend is in line with that of the maximum longitudinal displacement of the pier tops, because pier top displacements and pier base rotations are related to each other acknowledging the fact that pier top displacements were majorly caused by pier-base rotations and pier deformations. The reason for the reduction in these responses can be pier base rotation and pier deformation's complex combination with out-of-phase motion of the system.

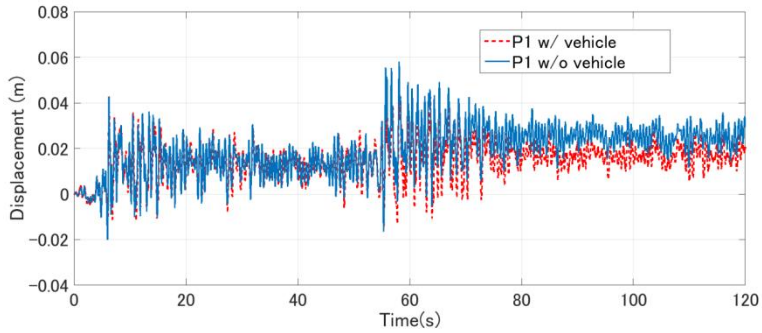

Figure 9: Longitudinal displacement responses of the pier top P1 under GM1.

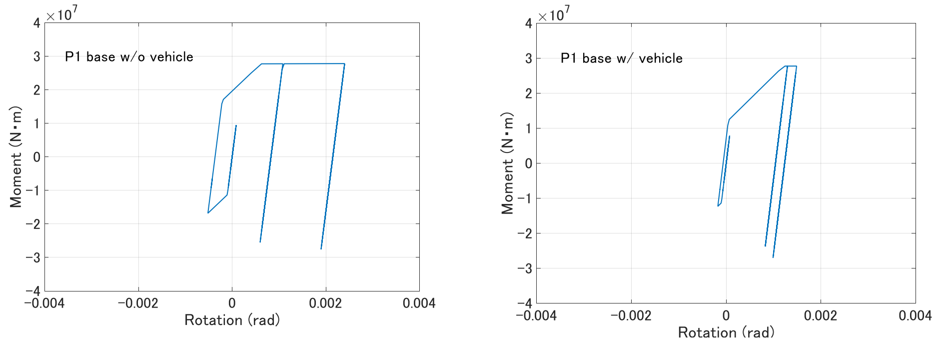

Figure 10: Hysteresis loop of plastic hinge at pier P1 base under GM1, disregarding moving vehicles (left) and considering moving vehicle (right).

Pier		Maximum displacement	Reduction ratio * %	Permanent displacement	Reduction ratio * %
Span center	w/o	0.166	1.8	0.014	21.4
	w/	0.163		0.011	
P1	w/o	0.058	13.8	0.025	31.6
	w/	0.050		0.017	
P2	w/o	0.066	19.3	0.031	35.9
	w/	0.053		0.020	

Note. *reduction ratio is defined as the average displacement reduction from the w/o-vehicles case to the w/-vehicles case divided by the average displacement in the w/o-vehicles case.

Table 8: Displacement responses of the bridge under GM1 (unit: m).

Pier		Rotation	Reduction ratio* %
P1	w/o	0.0024	37.5
	w/	0.0015	
P2	w/o	0.0028	39.3
	w/	0.0017	

Note. * reduction ratio is defined as the average rotation reduction from the w/o-vehicles case to the w/-vehicles case divided by the average rotation in the w/o-vehicles case.

Table 9: Maximum rotation of plastic hinge at pier base under GM1 (rad).

The hysteresis loop of bearing at P1 pier top and the longitudinal displacement responses of pier top under GM2 are depicted in Figures 11 and 12 as typical example, and those of A1, P2, A2 and the moment-rotation hysteresis loops at pier base are omitted here for simplicity. The maximum relative displacements of bearings considering VBI under GM2 increased up to 10% at A1, P1 and P2, but decreased slightly at A2 as indicated in Table 10. The maximum longitudinal displacements of pier tops were slightly reduced and the maximum displacement of span center was amplified a little, when the moving vehicles presented as shown in Table 11. The residual displacements of observation points were amplified by considering vehicle-bridge interaction up to 17% compared with those without considering vehicle-bridge interaction. Under strong ground motion GM2, the consideration of vehicle dynamics might yield larger longitudinal displacement and maximum relative displacement of bearing than those with bridge alone. The maximum rotation of the plastic hinge at pier base was reduced about 10% under moving vehicles compared with those with bridge alone subjected to GM2.

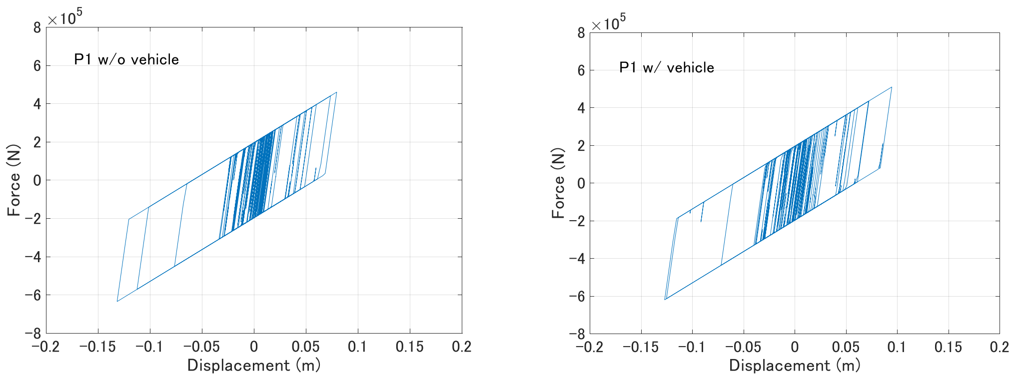

Figure 11: Hysteresis loop of bearing at P1 pier top under GM2, disregarding moving vehicles (left) and considering moving vehicle (right).

		Displacement	Reduction ratio * %
A1	w/o	0.403	-2.5
	w/	0.413	
P1	w/o	0.255	-9.4
	w/	0.279	
P2	w/o	0.240	-10.8
	w/	0.266	
A2	w/o	0.408	0.2
	w/	0.407	

Note. *reduction ratio is defined as the average displacement reduction from the w/o-vehicles case to the w/-vehicles case divided by the average displacement in the w/o-vehicles case.

Table 10: Maximum relative displacement of bearing under GM2 (unit: m).

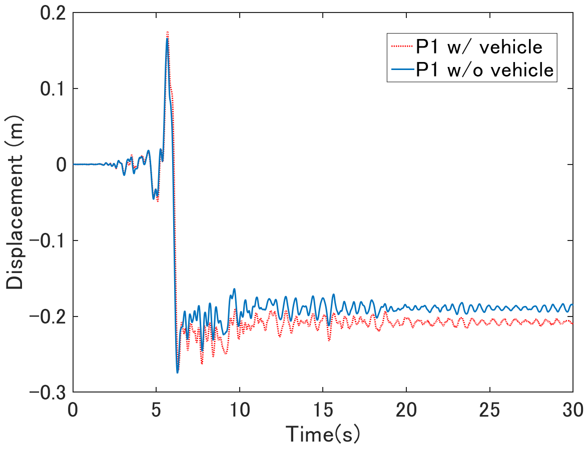

Figure 12: Longitudinal displacement responses of the pier top P1 under GM2.

Pier		Maximum displacement	Reduction ratio *%	Permanent displacement	Reduction ratio *%
Span center	w/o	-0.408	-1.0	-0.123	-17.1
	w/	-0.412		-0.144	
P1	w/o	-0.275	1.5	-0.189	-10.1
	w/	-0.271		-0.208	
P2	w/o	-0.285	1.4	-0.185	-8.6
	w/	-0.281		-0.201	

Note. *reduction ratio is defined as the average displacement reduction from the w/o-vehicles case to the w/-vehicles case divided by the average displacement in the w/o-vehicles case.

Table 11: Longitudinal displacement responses of the bridge under GM2 (unit: m).

Pier		Rotation	Reduction ratio*%
P1	w/o	-0.026298	10.1
	w/	-0.023652	
P2	w/o	-0.026038	9.7
	w/	-0.023504	

Note. * reduction ratio is defined as the average rotation reduction from the w/o-vehicles case to the w/-vehicles case divided by the average rotation in the w/o-vehicles case.

Table 12: Maximum rotation of plastic hinge at pier base under GM2 (unit: rad).

In general, in case of fully loaded traffic condition under strong earthquakes, ignoring vehicle effects would be on the non-conservative side. The vehicles had a significant negative effect on the bridge's nonlinear displacement responses.

5.2 Acceleration responses

Figure 13 shows the time history of the longitudinal acceleration observed at P1 pier top for example. The peak and RMS values of longitudinal acceleration responses of observation points are summarized in Figure 14.

From the peak and RMS values of longitudinal acceleration responses at span center and pier tops shown in Fig. 12, it is readily apparent that vehicles reduced the peak at span center and RMS values at span center and pier tops compared with that of disregarding vehicles, even if the peak values of acceleration responses at pier tops were amplified. The reduction in bridge acceleration could be explained by the relationship between the bridge's fundamental frequency and the response spectra of ground motions. The in-phase modes of the system were excited by the ground motions to cause the seismic responses of the bridge to a level lower than the original bridge-alone modes was. For example, in the pseudo acceleration response spectrum of the ground motion (Figure 6(c)), the spectral acceleration corresponding to the natural period (0.742 s, i.e. 1.348 Hz to the natural frequency) of the vehicle-bridge in-phase mode in Position 4 scenario, is smaller than that corresponding to the natural period (0.549 s, i.e. 1.822 Hz) of the bridge alone. The additional vehicle dynamics might move the system's fundamental period to a more favorable part of the spectrum where the spectral accelerations are less than the conventional case disregarding vehicle. Another reason may be the vehicles act as mass-spring-damper systems on the bridge. The natural period (0.549 s, i.e. 1.822 Hz) of the bridge alone and the longitudinal natural period (0.487 s, i.e. 2.052 Hz) of the vehicle are indicated in pseudo acceleration responses spectra of the ground motion in Fig. 6(c) and the vehicle and bridge would be excited by the ground motions. The vehicle resonated out of phase with the bridge motion and caused a phase difference in the bridge structural response, which affects the acceleration responses in way of a damper-like action.

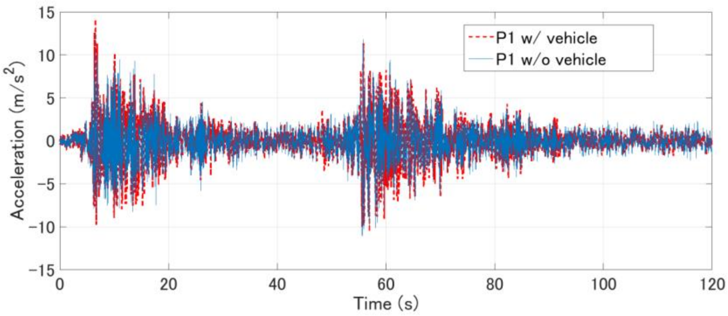

Figure 13: The time history of longitudinal acceleration responses of the bridge at pier top of P1 under GM1.

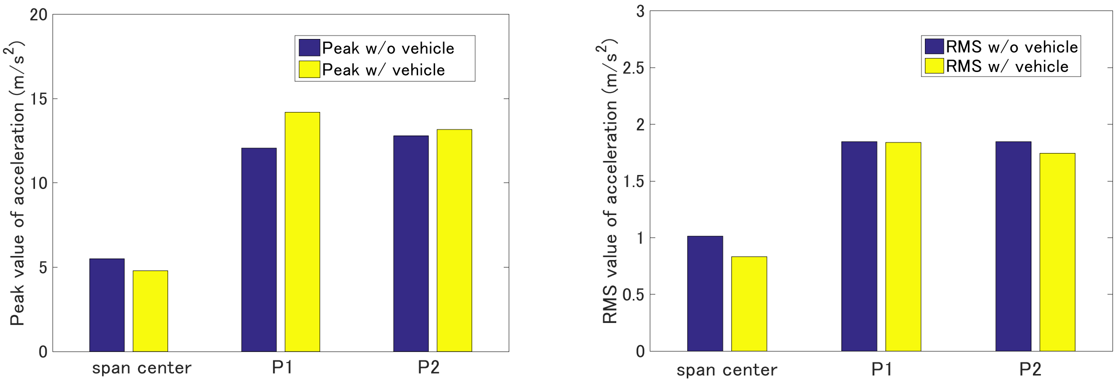

Figure 14: Peak (left) and RMS values (right) of longitudinal acceleration response of the bridge under GM1.

Figure 15 shows the time history of longitudinal acceleration responses of P1 pier top under GM2 as a typical example. Figure 16 shows the peak and RMS values of longitudinal acceleration responses of P1, P2 pier top and span center under GM2. As expected, they presented differently between the cases of regarding and disregarding moving vehicles. From the time histories, peak value and RMS values of longitudinal acceleration responses of observations points, it can be known that the longitudinal acceleration responses of the bridge generally decreased when the vehicles were considered in comparison with those when the vehicles were not considered. The observations presented herein showed that ignoring vehicle effects might be conservative when the acceleration responses were of concern.

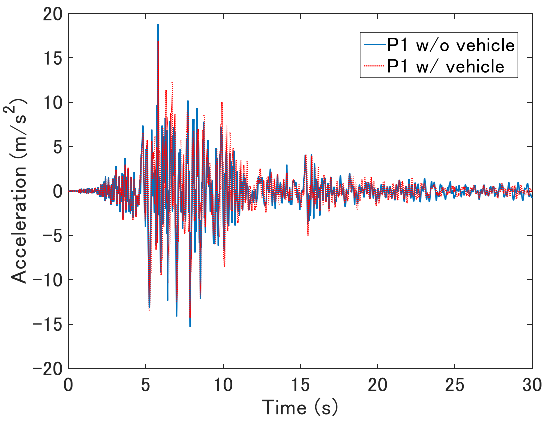

Figure 15: The time history of longitudinal acceleration response of P1 pier top under GM2.

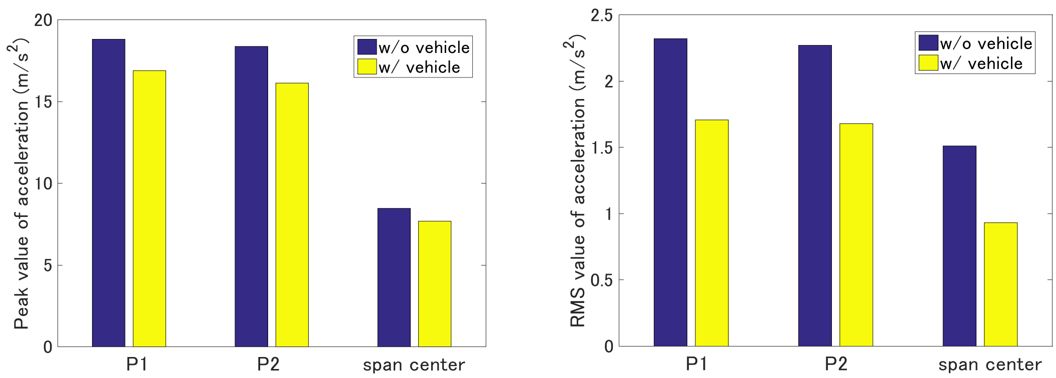

Figure 16: Peak (left) and RMS values (right) of longitudinal acceleration response of the bridge under GM2.

6 CONCLUSIONS

- In the longitudinal displacement, the presence of moving vehicles tends to reduce the maximum displacement and the permanent displacement under ground motion of Tohoku earthquake; reduce the maximum displacement and amplify the permanent displacement under ground motion of Kumamoto earthquake.
- In the bearing's relative displacement, the presence of moving vehicles tends to reduce the maximum displacement under ground motion of Tohoku earthquake, and amplify under ground motion of Kumamoto earthquake.

- The presence of moving vehicles reduced the RMS values of acceleration responses slightly even if increased the peak values of acceleration responses of bridge under ground motion of Tohoku earthquake;
- The results emphasized the need and importance of considering vehicle-bridge interaction as well as different ground motions in seismic design of bridges.
- The current assumption of ignorance of vehicle effect in seismic design of highway bridges might be non-conservative.

REFERENCES

[1] Japan Academic Network of Disaster Reduction, materials distributed in the press conference: http://janet-dr.com/11_saigaiji/160415kyushu_kaiken/160418all.pdf (retrieved: 04/22/2016).

[2] C.W. Kim, M. Kawatani, T. Kanbara, N. Nishimura, Seismic behavior of steel monorail bridges under train load during strong earthquakes. *Journal of Earthquake and Tsunami* , **7** (2), 1350006-1-1350006-17, 2013. DOI: 10.1142/S1793431113500061.

[3] H. Xia, M. Kawatani, T. Hayashikawa, T. Matsumoto, Numerical analysis on seismic response of Shinkansen bridge-train interaction system under moderate earthquakes. *Earthquake Engineering and Engineering Vibration*, **10** (1), 85-97, 2011. DOI: 10.1007/s11803-011-0049-1.

[4] Q. Zeng, E.G. Dimitrakopoulos, Seismic response analysis of an interacting curved bridge-train system under frequent earthquakes. *Earthquake Engineering & Structural Dynamics*, 45, 1129-1148, 2016. DOI: 10.1002/eqe.2699.

[5] C.W. Kim, M. Kawatani, Effect of train dynamics on seismic response of steel monorail bridges under moderate ground motion. *Earthquake Engineering & Structural Dynamics*, **35** (10), 1225-1245, 2006. DOI: 10.1002/eqe.580.

[6] I. Sugiyama, H. Kameda, N. Sasaki, S. Kawakita, Dynamic structure vehicle interaction of highway bridges and its implication to seismic design. *Proceedings of the 6th U.S.–Japan Bridge Engineering Workshop*, 379-392, Lake Tahoe, NV, 379-392May 7-8, 1990.

[7] H. Kameda, Y. Murono, A. Nanjou, N. Sasaki, Earthquake response of highway bridges under bridge-vehicle system. *Journal of Structural Mechanics and Earthquake Engineering JSCE (Doboku Gakkai Ronbushuu A)*, **626** (I-48), 93-106, 1999. (in Japanese)

[8] H. Kameda, H. Kita, H. Morikawa, Seismic load of highway bridges under dynamic effect of vehicle loading. *Journal of Structural Engineering*, 36 A, 791-801, 1990. (in Japanese)

[9] C.W. Kim, M. Kawatani, S. Konaka, R. Kitaura, Seismic responses of a highway viaduct considering vehicles of design live load as dynamic system during moderate earthquakes. *Structure and Infrastructure Engineering,* **7**(7-8), 523-534, 2011.DOI: 10.1080/15732479.2010.493339.

[10] M. Kawatani, C.W. Kim, K. Iwashita, K. Yasui, Seismic Responses of Highway Viaducts Incorporating Bridge-Vehicle Interaction. *Journal of JSCE A*, **64** (4), 678-691, 2008. (in Japanese)

[11] S. Borjigin, C.W. Kim, K.C. Chang, K. Sugiura, Nonlinear dynamic response analysis of vehicle–bridge interactive system under strong earthquakes. *Engineering Structures*, 176, 500-521, 2018. https://doi.org/10.1016/j.engstruct.2018.09.014

[12] R.W. Clough, J. Penzien, *Dynamics of Structures*. New York, McGraw Hill, 2003.

[13] ISO 8608: Mechanical vibration—Road surface profiles—reporting of measured data. *International Organization for Standardization*, 1995(E).

[14] *Design specification of highway bridges. Part V: Seismic design*. Japan Road Association, Japan, 2012.

[15] Earth Science and Disaster Prevention (NIED). (Available from: http://www.kyoshin.bosai.go.jp/kyoshin/) accessed on [24 August 2016].

[16] C.W. Kim, M. Kawatani, K.B. Kim, Three-dimensional dynamic analysis for bridge-vehicle interaction with roadway roughness. *Computer and Structures*,**83**,1627-1645, 2005. DOI:10.1016/j. compstruc. 2004.12.004.

[17] A. Gonzalez, Vehicle–bridge dynamic interaction using finite element modelling. *Finite Element Analysis*, *Moratal*, D. (Ed.), ISBN: 978-953-307-123-7, InTech, 2010. DOI: 10.5772/10235.

[18] S. Borjigin, C.W. Kim, K.C. Chang, K. Sugiura, Numerical investigations on dynamic responses of a highway bridge under moving vehicles subject to strong earthquakes. *Proceedings of JSCE Annual Conference*, Sendai, Japan, September 7-9, 2016.

[19] L.M. Anggraini, S. Borjigin, C.W. Kim, K. Sugiura, Seismic response analysis of urban highway viaducts under multiple vehicles subjected to strong earthquakes. *16th World Conference on Earthquake Engineering*, Santiago Chile, January 9-13, 2017.